



Published in final edited form as:

J Orthop Res. 2021 March ; 39(3): 506–515. doi:10.1002/jor.24836.

Longitudinal Analysis of the Contribution of 3D Patella and Trochlear Bone Shape on Patellofemoral Joint Osteoarthritic Features

Tzu-Chieh Liao, PT, PhD¹, Hannah Jergas, MD¹, Radhika Tibrewala, MSc¹, Emma Bahroos, MSc¹, Thomas M. Link, MD, PhD¹, Sharmila Majumdar, PhD¹, Richard B. Souza, PT, PhD^{1,2}, Valentina Pedoia, PhD¹

¹Department of Radiology and Biomedical Imaging, University of California-San Francisco, San Francisco, CA, USA

²Department of Physical Therapy and Rehabilitation Science, University of California-San Francisco, CA, USA

Abstract

To explore bone shape features that are associated with patellofemoral joint (PFJ) osteoarthritic features. Thirty subjects with PFJ degeneration (6 males, 53.2 ± 9.8 years) and 23 controls (12 males, 48.1 ± 10.6 years) were included. Magnetic resonance (MR) assessment was performed to provide bone segmentation, morphological grading, and cartilage relaxation times. Additionally, subject self-reported symptoms were reported. Logistic regressions were used to identify the shape features that were associated with the presence and worsening of PFJ morphological lesions over 3 years, and worsening of self-reported symptoms. Statistical parametric mapping was used to evaluate the associations between shape features and cartilage relaxation times at 3 years. Results indicated that subjects with PFJ degeneration exhibited a trochlea with longer lateral condyle and shallower trochlear groove (adjusted OR = 0.30, 95% CI: 0.10, 0.86; $p = 0.025$). Subjects with worsening of PFJ degeneration exhibited a patella with equally distributed facets (adjusted OR = 3.14, 95% CI: 1.05, 9.37; $p = 0.040$) and lateral bump (adjusted OR = 0.14, 95% CI: 0.02, 0.83; $p = 0.030$). No shape features were associated with worsening of self-reported symptoms. Elevated $T_{1\rho}$ and T_2 times at 3 years were associated with a patella with a lateral hook, equally distributed facets, round and thick as well as a trochlea larger in size ($R = 0.38\sim 0.46$, $p = 0.015\sim 0.025$).

The study demonstrated the ability of 3D statistical shape modeling to quantify patella and trochlear bone shape features that are associated with the presence and progression of PFJ osteoarthritic features.

Correspondence Address: Tzu-Chieh Liao, Department of Radiology and Biomedical Imaging, University of California-San Francisco, San Francisco, 185 Berry Street, Lobby 6, Suite 350, San Francisco, CA 94710, USA, Phone: 415-476-1000, tzu-chieh.liao@ucsf.edu.

Author Contributions Statement

Liao and Jergas have substantial contributions to drafting the manuscript, while Souza and Pedoia revised it critically. Liao, Jergas, Tibrewala, and Bahroos contributed to the acquisition, analysis, or interpretation of the data. Finally, all authors contributed to the approval of the submitted and final versions.

Keywords

bone shape; osteoarthritis; patellofemoral; statistical shape modeling

Introduction

Knee osteoarthritis (OA) is a major health concern worldwide and a leading cause of disability in adults. Even though knee OA can affect both of the tibiofemoral joint (TFJ) and patellofemoral joint (PFJ), most research data are available for TFJ OA alone.^{1, 2} Interestingly, some reports revealed that perhaps PFJ OA is even more prevalent than TFJ OA.^{3, 4} Based on a radiographic study, the distribution of compartmental OA in adults aged 50 year and above with knee pain were 40% for combined TFJ and PFJ, 24% for isolated PFJ, and 4% for isolated TFJ.³ In a review of large community-based studies, the prevalence of PFJ OA was 38% and 44% based on radiographic and magnetic resonance (MR) findings in adults, respectively.⁵

Morphological changes in cartilage in the early stages of OA include a failure to synthesize the extracellular matrix components, loss of proteoglycans, collagen and thus elasticity and reduction in water content.⁶ Quantitative MR imaging offers tools to probe the biochemical composition of articular cartilage. $T_{1\rho}$ and T_2 relaxation times are related to the proteoglycan content and collagen orientation of the cartilage and can thus provide information on the state of cartilage health.⁷ Elevated $T_{1\rho}$ and T_2 relaxation times have been associated with the development of knee OA^{8, 9} and may present biomarkers for early cartilage degeneration.¹⁰ In particular, Teng et al. has shown elevated $T_{1\rho}$ and T_2 relaxation times in individuals with PFJ OA when compared to controls.¹¹ Additionally, MR imaging offers morphological assessment of the soft tissues such as cartilage lesions and bone marrow edema-like lesions (BMELs).^{12, 13} A well-established grading system, the whole organ MR imaging score (WORMS),^{12, 13} has been widely used to characterize morphological lesions/abnormalities of the knee joint structures, including the PFJ compartments. Taken together, MR imaging offers the tools to assess early OA-related changes longitudinally.

While OA is often primarily identified as a degeneration of the articular cartilage, it has also been stated that certain bone shape features may present increased risk for the development of OA.^{14–16} In the TFJ, Neogi et al.¹⁶ has reported that widening and flattening of the femoral and tibial condyles are associated with the radiographic incidence of knee OA. On the other hand, research has reported that trochlear morphology, such as decreased trochlear inclination angle and decreased sulcus angle, are associated with worsening of PFJ OA features.^{14, 15} While the influence of trochlear morphology and patella alignment have been widely studied on PFJ OA,^{14, 17, 18} little is known regarding the influence of patella morphology.¹⁹

While direct measures of geometrical properties, such as sulcus angle or joint alignment, have the great advantage of a clear physical interpretation and can be easily performed by clinicians, they are usually hypothesis-driven, limiting a full spatial analysis. In the last few years, data driven statistical methods which offer a more comprehensive and unbiased

description of bone morphology have emerged. For instance, statistical bone shape modeling provides the non a-priori features selection of bone shape, which may aid in identifying clinically significant bone shape features that have been previously overlooked. Several studies have used 2D modeling based on radiographs to quantify bone geometry.^{20, 21} In recent years, with the use of MR imaging, more and more studies have conducted 3D bone shape analyses using Statistical Shape Modeling.^{16, 22} The 3D method provides a more comprehensive understanding of shape features than 2D analyses which are limited from the 3D complexity of the bone shape and could potentially be affected by joint positioning during scanning.

Even though a consistent body of research already exists that links bone shape and idiopathic knee OA,^{16, 22} no conclusive longitudinal studies have been performed with the aim of establishing a correlation between 3D patella and trochlear bone shape features with longitudinal changes of PFJ OA, both morphologically and symptomatically. Therefore, the aim of this study is twofold: (i) to explore bone shape features that are associated with the presence of PFJ degeneration, defined as morphological lesions of the trochlea and patella; (ii) to identify whether bone shape features predict worsening of PFJ OA-related changes over 3 years, defined as morphological joint lesions, self-reported symptoms, and compositional cartilage changes (prolongation of $T_{1\rho}$ and T_2 relaxation times).

Methods

Subjects

Thirty subjects with the presence of isolated PFJ degeneration (sex, 6 males; age, 53.2 ± 9.8 years; body mass index (BMI), 23.8 ± 3.2 kg/m²) and 23 controls (12 males, 48.1 ± 10.6 years, 23.9 ± 3.0 kg/m²) from a longitudinal cohort on knee OA were included in this study. Subjects above 35 years with and without knee OA symptoms were recruited from the community. Presence of PFJ degeneration was defined as cartilage and/or BMELs identified either at the patella or trochlea, or both, using a MR-based semi-quantitative morphological grading system, WORMS grading,^{12, 13} which is described in details later. Subjects were excluded if any of the following criteria were present: (i) age under 35 years, (ii) presence of TFJ degeneration as shown on WORMS grading, (iii) history of lower extremity or spine surgery, (iv) self-reported inflammatory arthritis, and (v) contraindications to MR imaging. The study was approved by the Committee of Human Research at the University of California, San Francisco (UCSF) and prior to data collection, all subjects signed a written informed consent. All subjects received baseline assessment and were invited for follow-up at 3 years. The level of evidence of the current study was Level 3.

MR Imaging Assessment

All subjects underwent unilateral knee MR imaging using a 3.0T GE MR scanner (General Electric, Milwaukee, WI, USA) with a quadrature 8-channel transmit and receive knee coil (Invivo, Inc., Gainesville, FL). All subjects were positioned in a supine position with the knee in neutral rotation and full extension. To reduce motion artifacts, the foot of the subject was secured in place, the study knee was stabilized with padding, and a belt was secured across the patient's waist. Subjects arrived at the imaging center and were

unloaded (seated in a chair) for a 45 min period, after which the following sequences were acquired: (i) sagittal high-resolution intermediate-weighted fast-spin echo (FSE) CUBE sequence for clinical morphological grading and cartilage segmentation (repetition time (TR)/echo time (TE) = 1500/26.69 ms, field of view (FOV) = 16 cm, matrix = 384 × 384, slice thickness = 0.5 mm, echo train length = 32, bandwidth = 37.5 kHz, number of excitations = 0.5, acquisition time = 10.5 min), (ii) T_{1ρ} relaxation time sequence (TR/TE = 9/2.6 ms, time of recovery = 1500 ms, FOV = 14 cm, matrix = 256 × 128, slice thickness = 4 mm, bandwidth = 62.5 kHz, time of spin-lock (TSL) = 0/2/4/8/12/20/40/80 ms, frequency of spin-lock = 500 Hz, acquisition time = 11 min), (iii) the T₂ relaxation time sequence (same as the T_{1ρ} quantification except for magnetization preparation TE = 1.8/3.67.3/14.5/29.1/43.6/58.2, acquisition time = 11 min), and (iv) sagittal fat-saturated T2 FSE images for bone segmentation (TR/TE = 4000/49.3ms, FOV = 16 cm, matrix = 512 × 512, slice thickness = 1.5 mm, echo train length = 9, acquisition time = 2.5 min).

MR-Based Morphological Grading

Cartilage and bone marrow morphological abnormalities of the patella and trochlea were graded by an experienced board-certified radiologist on the FSE CUBE MR sequences using the WORMS grading,^{12, 13} which was previously shown to provide high intra- and inter-reader agreements (intra: 95.1%, inter: 95.3%).²³ Cartilage lesions were graded using a 8-point scale: 0 = normal thickness, 1 = normal thickness, increased signal intensity, 2 = partial thickness focal lesion less than 1 cm of greatest width, 2.5 = full thickness focal lesion less than 1 cm of greatest width, 3 = multiple areas partial lesion less than 1 cm of greatest width, or grade 2 lesion wider than 1 cm but less than 75% of the region, 4 = diffuse partial thickness loss greater than 75% of the region, 5 = multiple areas of full thickness lesion greater than 1 cm but less than 75% of the region, and 6 = diffuse full thickness loss greater than 75% of the region. The BMELs were graded using a 4-point scale: 0 = none, 1 = <25% of the subregion, 2 = 25~50% of the subregion, 3 = >50% of the subregion. Presence of PFJ degeneration at baseline was defined if the patella and/or trochlea demonstrated WORMS for cartilage lesions greater or equaled to 2 and/or BMELs greater or equaled to 1. At follow-up, longitudinal assessment of WORMS grading was performed to determine if the subjects demonstrated worsening of PFJ lesions. Subjects were stratified as morphological progressors if changes in WORMS grading for either cartilage lesions or BMELs from baseline to 3 years were greater than or equaled 1,^{24, 25} otherwise they were classified as non-progressors.

Self-Reported Symptoms

All subjects were required to complete the self-administrated Knee Injury and Osteoarthritis Outcome Score (KOOS) at each assessment. The KOOS questionnaire consists of five subscales: pain, other symptoms, function in daily living, function in sport and recreation, and knee related quality of life.²⁶ A normalized score (100 indicating no symptoms and 0 indicating extreme symptoms) was calculated for each subscale.

All subjects were stratified into symptomatic progressors and non-progressors based on changes in KOOS over 3 years. In the current study, we specifically chose the KOOS subscales of pain and other symptoms to represent progression. Raw changes in each

subscore from baseline to 3 years were quantified to determine if subjects demonstrated worsening of scores at follow-up. Subjects were defined as symptomatic progressors if the worsening in either pain and other symptom subscores at follow-up exceeded the minimal detectable change score from the literature. The minimal detectable change scores from the literature are 13.4 for pain and 15.5 for other symptoms, respectively.^{27, 28}

Voxel-Based Relaxometry

Image post-processing for obtaining VBR was performed in MATLAB integrated with Elastix registration toolbox for non-rigid image registration.^{29, 30} The details of the process have been previously described.³¹ A single reference image was identified through an iterative process aimed to minimize the global image deformation. All images were then non-rigidly registered and aligned to the single reference image. Relaxation maps were computed in a voxel-by-voxel basis by fitting the morphed images from different TSLs or TEs, for $T_{1\rho}$ or T_2 respectively, employing Levenberg-Marquardt mono-exponentials applied to each voxel ($S(\text{TSL}) \propto \exp(-\text{TSL}/T_{1\rho})$).

Bone Shape Analysis

All image post-processing was performed with in-house programs written in MATLAB (MathWorks, Natick, MA). Segmentation was first performed for patella and femur bones semi-automatically through edge detection with a three-dimensional smoothness constraint through Bezier interpolation.^{32, 33}

Marching Cube algorithm was used to extract the three-dimensional triangulated mesh of bone, then applying a Laplacian smoothing to the mesh. Analyses of the patella and femur were performed separately, independent to the relative position of the joint. Each subject bone surface was rigidly registered on a reference template identified in the dataset. Surface landmark matching was performed using an algorithm suggested by Lombart et al.³⁴ Maximum and minimum local curvatures were used for coupling homologous points on two surfaces as previously described.³⁵ Both were locally defined on the surfaces and used to identify the landmark matching solved using Coherent point drift. We identified landmarks on the surface, each landmark was described by a set of 3D coordinates. These coordinates can be considered as points in a $3*L$ dimension space with L being the total number of landmarks.

Eigen vector decomposition was then used for principal component analysis on the covariance matrix to extract the most important modes of variation of the bone shape. The effect of each mode, called principal component (PC), that represents independent bone shape features can be modeled individually, by changing the value of each mode from the mean, to the mean ± 3 mode variance. Clinical interpretation of each PC mode can then be investigated by observing the 3D surfaces. The process was performed individually for patella and trochlea. The first 5 PCs, that described the majority of the overall variation, were subsequently outlined for their clinical interpretation and considered for further analysis. Model reliability for this method is known to be excellent.³⁵

Statistical Analysis

Chi-square and independent *t* tests were used to compare demographics between the PFJ degeneration and control groups, as well as progressors and non-progressors at follow-up. Mann-Whitney U test was used to perform group comparisons for KOOS as the distribution of KOOS was skewed. Standard logistic regression models were used to identify the possible bone shape features that were associated with the presence of PFJ degeneration at baseline, the worsening of WOMBS grading over 3 years, and the worsening of KOOS over 3 years, with the covariates of sex, age, and BMI.

Statistical parametric mapping was used to evaluate the associations between bone shape features at baseline and cartilage relaxation times at 3 years using Pearson partial correlations on a voxel-by-voxel basis. Percentage of voxels showing significant correlation (PSV), average correlation coefficient (*r*) of voxels showing significant correlation, and average *p* values of voxels showing significant correlation were reported from the statistical parametric mappings. Only results with PSV more than 10% of the voxels were considered to provide more clinically significant patterns.³⁶ Random Field Theory correction was used to take into account possible false positives due to multiple comparison.³⁷ The analyses were carried out with the covariates of sex, age, BMI. To account for cartilage relaxation times at baseline, $T_{1\rho}$ or T_2 relaxation times computed as an average of all voxels within the patella and trochlear cartilages were used as covariates. The alpha value was set at 0.05.

Results

Demographics

Baseline subject characteristics are presented in Table 1. Significant group differences were found for sex ($p = 0.020$) between the PFJ degeneration and control groups. No group differences were found for age, BMI, and subject self-reported symptoms (KOOS). Distribution of WOMBS grading in the PFJ degeneration group is presented in Figure 1. Of all the 30 subjects that exhibited PFJ morphological lesions at baseline, only one subject exhibited isolated BMELs, while the remainings exhibited cartilage lesions. Additionally, lesions at the patella appeared to be more prevalent than trochlea. At 3 years, a total of 48 (90.5%) subjects returned for the follow-up and only the returned subjects were included in the longitudinal analyses.

Based on the changes in PFJ morphology, 22 subjects (2 males, 54.7 ± 10.1 years, 24.5 ± 3.7 kg/m²) exhibited worsening of WOMBS grading in either cartilage lesions or BMELs, and were further stratified as morphological progressors, with the remaining 26 subjects (16 males, 48.7 ± 10.5 years, 23.4 ± 2.4 kg/m²) as morphological non-progressors. A significant group difference was found for sex ($p < 0.001$), as more females were stratified as morphological progressors, and there was a trend towards older age in the progressor group ($p = 0.052$).

Based on changes in self-reported symptoms, 7 subjects (3 males, 53.2 ± 10.7 years, 25.0 ± 3.1 kg/m²) exhibited worsening of either KOOS-pain or other symptom subscores, with the remaining 41 subjects (15 males, 51.1 ± 10.7 years, 23.7 ± 3.1 kg/m²) as symptomatic non-progressors. No group differences were found in any demographic variables.

Bone Shape Features

The first 5 modes from patella bone shape analysis described 65.2% of the overall variation within the dataset and were considered for further analysis (Figure 2). Mode 1 alone described 22.9% of the total variability within the dataset. Modeling of PC1 revealed that lower PC1 corresponded to a patella with a dominant lateral facet; on the contrary, higher PC1 corresponded to equally distributed medial and lateral facets. Modeling of PC2 (16.3%) revealed that lower PC2 corresponded to a greater facet angle. Modeling of PC3 (10.3%) revealed that lower PC3 corresponded to a patella with a lateral bump or hook. Modeling of PC4 (8.7%) revealed that lower PC4 corresponded to a patella with lower width. Lastly, modeling of PC5 (6.8%) revealed that lower PC5 corresponded to a wide and shallow patella as opposed to round and thick.

The first 5 modes from trochlear bone shape analysis described 72.8% of the overall variation (Figure 3). Modeling of PC1 (26.0%) suggested a width effect, as lower PC1 corresponded to a trochlea with greater intercondylar width. Modeling of PC2 (18.7%) suggested a size effect as lower PC2 corresponded to a smaller trochlea. Modeling of PC3 (13.1%) revealed that lower PC3 corresponded to a trochlea with a longer lateral condyle and shallower trochlear groove as opposed to longer medial condyle and deeper groove. Modeling of PC4 (8.8%) revealed that lower PC4 corresponded to greater lateral trochlear inclination angle and narrowing of intercondylar notch. Modeling of PC5 (5.9%) revealed that lower PC5 corresponded to a smaller trochlea in size and deeper intercondylar notch.

Baseline Analysis

Logistic regression that examined the bone shape features that were associated with the presence of PFJ morphological lesions at baseline revealed that trochlear PC3 (adjusted odds ratio [OR] = 0.30, 95% confidence interval [CI]: 0.10, 0.86; $p = 0.025$) and sex (adjusted OR = 15.66, 95% CI: 2.16, 113.42; $p = 0.006$) were significant features. Based on the OR, it demonstrated that PFJ degeneration group exhibited lower PC3, that is, subjects with PFJ degeneration demonstrated a trochlea with a longer lateral condyle and shallower trochlear groove as compared to subjects without PFJ degeneration (Figure 3). No patella mode was found to be associated with the presence of PFJ degeneration at baseline.

Longitudinal Analysis

Logistic regression that examined the predictor(s) of the worsening of PFJ morphological lesions over 3 years revealed patella PC1 as a significant predictor (adjusted OR = 3.14, 95% CI: 1.05, 9.37; $p = 0.040$), as morphological progressors exhibited a patella with equally distributed medial and lateral facets as opposed to a dominant lateral facet as in non-progressors. The same regression model revealed patella PC3 as another significant predictor (adjusted OR = 0.14, 95% CI: 0.02, 0.83; $p = 0.030$), as morphological progressors exhibited a patella with a lateral bump or hook. Sex was again a significant predictor (adjusted OR = 23.45, 95% CI: 2.35, 234.01; $p = 0.007$). No trochlear mode was found to be a predictor of the worsening of PFJ morphological lesions longitudinally. Lastly, logistic regression that examined the predictor(s) of the worsening of self-reported symptoms over 3 years revealed that no bone shape features were a significant predictor.

In assessment of the associations between longitudinal cartilage relaxation times and bone shape features, results of the statistical parametric mappings revealed that elevated $T_{1\rho}$ was associated with lower patella PC3 score, resembling a patella with a lateral bump of hook (trochlea region, PSV = 10.2%, average $R = -0.39$, average $p = 0.020$) (Figure 4a) and greater trochlear PC2 score, resembling a trochlea larger in size (patella region, PSV = 12.8%, $R = 0.38$, $p = 0.025$) (Figure 4b). Elevated T_2 was associated with greater patella PC1, resembling equally distributed medial and lateral facets (patella region, PSV = 10.5%, $R = 0.43$, $p = 0.019$) (Figure 4c) and greater patella PC5 scores, resembling a round and thick patella (trochlea region, PSV = 13.3%, $R = 0.46$, $p = 0.015$) (Figure 4d).

Discussion

In this study, we found significant associations between patella and trochlear bone shape features with presence and progression of PFJ osteoarthritic features. Subjects with PFJ degeneration exhibited a trochlea with shallower trochlear groove, while subjects demonstrating worsening of PFJ lesions exhibited a patella with equally distributed facets and lateral bump. A correlation between bone shape features and the onset of OA has been described in the literature before. However, it has thus far remained unclear whether patella and trochlear bone shape features may be predictive for the development of PFJ OA.

The trochlear bone shape features globally describe the surface, such as the depth, intercondylar space of trochlear groove, and length of femoral condyles. As for the patella, the features in general describe the ratio between medial-lateral facets in area, angle, as well as the length and depth of the patella globally. In the current study, we opted to retain the first 5 modes for further analysis due to several concerns. First, the selected modes overall explained moderate variation in the dataset (65~72%) that were comparable to previous studies,^{35, 38} additionally allowing us to investigate the more easily interpretable features. Further, from a statistical standpoint, it is advised that 10 subjects per variable are required in a regression analysis, suggesting that 5 predictor variables per model will be appropriate with a sample size of 53 subjects as included in the current study. The strength of principal component analysis especially lies in the non a-priori features selection as well as full spatial analysis of the bone. Our approach using Statistical Shape Modeling on 3D MR imaging appears to be effective in characterizing patella and trochlear bone shape features that are associated with PFJ OA-related degeneration.

Femoral trochlear morphology has been previously associated with PFJ pathology and may underlie the development and progression of PFJ OA. Trochlear dysplasia, characterized as decreased sulcus angle and lateral trochlear inclination, has been related to patella degeneration and decreased patella cartilage volume.³⁹ Based on the results of the adjusted ORs, every 1 SD increase in trochlear PC3 is related to a 0.3 times lower occurrence of PFJ degeneration, which a positive trochlear PC3 resembles a deeper trochlear groove (Figure 3, trochlea – mode 3). In other words, a deeper trochlear groove has a protective effect on the incidence of PFJ degeneration, suggesting a consistent result with previous findings.³⁹ Literature has shown that a shallow trochlear groove can result in patella malalignment and maltracking as previously suggested.⁴⁰ Further, patella malalignment and maltracking lead to decreased PFJ contact area,⁴¹ and thus, elevate joint stress at the articular surface.⁴²

In turn, it can lead to PFJ articular cartilage lesions⁴³ and knee pain.⁴⁴ Apart from the shape of trochlear groove, our results suggest the significance of a longer lateral condyle in the anterior-posterior direction (trochlea – mode 3). This feature has not been previously reported to be associated with PFJ pathology; nevertheless, we speculate that a longer lateral condyle may influence TFJ kinematics, which again, lead to changes in PFJ stress.^{45, 46} Taken together, our results confirm that trochlear shape, such as a shallow groove, is associated with the presence of PFJ OA.

In our longitudinal analysis, we found two relevant patella modes that predicted the worsening of cartilage lesions and BMELs over 3 years. The first positive mode was characterized as a patella with equally distributed medial and lateral facets (Figure 2, patella – mode 1). Every 1 SD increase in patella PC1 is related to 3.1 times greater odds of worsening of PFJ morphological lesions over 3 years. That is, equally distributed medial and lateral facets are associated with higher risks of PFJ morphological progression. It should be noted that typically, the patella has a dominant lateral facet (greater in area).⁴⁷ A smaller patella lateral facet leads to a decrease in contact area, further elevating joint stress on the lateral facet, coinciding where PFJ pathology is commonly observed. The second mode that predicted worsening of PFJ morphological lesions was characterized as a patella with a lateral bump or hook (Figure 2, patella – mode 3). Every 1 SD increase in patella PC3 (without lateral bump) is related to 0.14 times less likely of worsening of PFJ morphological lesions over 3 years. On examination of this particular shape feature on MR images, the bump or hook may resemble an osteophyte or exostosis (Figure 5). It is possible that the osteophyte appearance is a coexisting feature of PFJ morphological degeneration rather than a risk factor towards the worsening of PFJ lesions.

On the contrary, no patella nor trochlear bone shape features were associated with the progression of subject self-reported symptoms over 3 years. This is consistent with a previous study that reported no associations between trochlear shape and symptoms in persons with patellofemoral pain.⁴⁸ To the best of our knowledge, no study has reported the association between symptoms and patella bone shape since most studies have focused on patella alignment measures. Nevertheless, two confounding factors that should be noted when interpreting the results. First, of the 48 subjects analyzed, only 7 subjects (14.5%) exhibited symptomatic progression over 3 years. The small sample size is subjected to the likelihood of type II error. Second, KOOS is a measure of overall knee symptoms but not specifically designed for PFJ. Additionally, it may not be a sensitive tool to detect symptomatic progression given the high minimal detectable change scores. Recently, a modified KOOS specially designed for individuals with patellofemoral pain and PFJ OA has been developed (KOOS-PF).⁴⁹ Future study should focus on the assessment of KOOS-PF to better identify PFJ OA symptomatic progression.

In addition to the longitudinal assessment of bone shape and worsening of morphological lesions and self-reported symptoms, the associations between bone shape and cartilage relaxation times were examined. Similar to the aforementioned results, a patella with equally distributed medial and lateral facets, as well as a patella with a lateral bump were found to be associated with elevated $T_{1\rho}$ and T_2 relaxation times at 3 years. Furthermore, a rounder and thicker patella was associated with elevated T_2 relaxation times in the femoral cartilage

region longitudinally (patella – mode 5). Lastly, we found that a larger trochlea in size was associated with elevated T₂ relaxation times as well (trochlea – mode 2). However, this feature has not been reported to associate with OA, the mechanistic relationship between trochlear size and degeneration is currently unknown. Cartilage relaxation times are imaging biomarkers that have been found to be sensitive to the compositional changes in cartilage associated with early OA.¹⁰ Taken together, our results suggested that, as a future direction, the combination of shape and cartilage compositional analyses aid to the prediction of OA development and progression.

The influence of patella bone shape on PFJ OA has not been well studied, as most studies have focused on patella position relative to the femur, using metrics such as bisect offset, patella tilt angle, and length ratio.⁴³ Few studies that have examined patella bone shape were limited to 2D radiography analysis, with one study reporting no influence of patella width, thickness, and medial-lateral facet angle on PFJ cartilage lesions.⁵⁰ On the other hand, our results were consistent with Eijkenboom et al.¹⁹ who used similar Statistical Shape Modeling on 2D radiograph. The authors reported that individuals with patellofemoral pain and PFJ OA exhibit a patella with equally distributed medial and lateral facets as well as a rounder inferior-posterior patella, both of which were found to be associated with longitudinal worsening of PFJ morphological lesions in the current study.

Our findings aid to the current knowledge between bony anatomy and a higher risk of PFJ OA, and understanding the factors that place certain individuals to higher risk of OA allows early screening and detection. Even though risk factors associated with bony anatomy may not be modifiable, the identified subjects should be targeted for prevention strategy including education and training. In the current study, we identified several clinically accessible measures that are associated with PFJ OA. Additionally, the targeted bone shape features that we identified were distinct from the commonly assessed alignment measures (i.e. patella lateral displacement, lateral tilt). These bone shape features such as facet distribution and a round patella, even though identified from 3D MR imaging, can be easily examined on 2D clinical images.

Despite the promising results reported in the current study, some limitations need to be acknowledged. First, it should be noted that an uneven sex distribution was presented in the subject demographic (18 males vs. 30 females). This was due to the gender biased in the natural prevalence of PFJ OA as females tend to have a higher prevalence rate, and that the subjects were selected based on the presence of PFJ degeneration, excluding those with TFJ degeneration. We acknowledged the bias and considered sex as a covariate in all our statistical analyses to minimize the effect. Second, we are interested in the contribution of patella and femur bone shape to PFJ OA, therefore our interpretation was mainly focused on the articulating surface of PFJ (patella and trochlea). Other features such as the length of femoral shaft, shape of the femoral condyles were not considered. Nevertheless, it is believed that patella facets and femoral trochlea play more significant roles to PFJ pathology as compared to other features. Lastly, the MR-based analysis greatly depends on the resolution of the images. If better acquisition and reconstruction were provided, it would allow the analysis of more localized shape features ranked in later modes that may not have been considered as part of the current study.

In conclusion, the study demonstrated the ability of 3D Statistical Shape Modeling to characterize and quantify patella and trochlear bone shape features from MR imaging, that were associated with the presence and progression of PFJ degeneration. On the contrary, bone shape features were not associated the progression of subject self-reported symptoms. While the results were consistent with previous literature, several new findings warrant larger study and longer follow-ups. For instance, the length of the condyles as well as patella and trochlear size were found to be associated with PFJ degeneration, which have not been reported. Nevertheless, the insights presented in the current study provided new information regarding the associations between patella and femur bone shape with PFJ cartilage degeneration, suggesting that MR-based bone shape modeling may be a promising imaging biomarker for the study of early PFJ OA.

Acknowledgements

Funding was from NIH-NIAMS R01 AR062370, NIH-NIAMS R01 AR069006, and NIH-NIAMS K24 AR072133.

References

1. Arokoski JP, Jurvelin JS, Vaatainen U, Helminen HJ. Normal and pathological adaptations of articular cartilage to joint loading. *Scand J Med Sci Sports*. 2000;10:186–198. [PubMed: 10898262]
2. Bennell KL, Bowles KA, Wang Y, Cicuttini F, Davies-Tuck M, Hinman RS. Higher dynamic medial knee load predicts greater cartilage loss over 12 months in medial knee osteoarthritis. *Ann Rheum Dis*. 2011;70:1770–1774. [PubMed: 21742637]
3. Duncan RC, Hay EM, Saklatvala J, Croft PR. Prevalence of radiographic osteoarthritis--it all depends on your point of view. *Rheumatology (Oxford)*. 2006;45:757–760. [PubMed: 16418199]
4. Szebenyi B, Hollander AP, Dieppe P, et al. Associations between pain, function, and radiographic features in osteoarthritis of the knee. *Arthritis Rheum*. 2006;54:230–235. [PubMed: 16385522]
5. Hart HF, Stefanik JJ, Wyndow N, Machotka Z, Crossley KM. The prevalence of radiographic and MRI-defined patellofemoral osteoarthritis and structural pathology: a systematic review and meta-analysis. *Br J Sports Med*. 2017;51:1195–1208. [PubMed: 28456764]
6. Cucchiari M, de Girolamo L, Filardo G, et al. Basic science of osteoarthritis. *J Exp Orthop*. 2016;3:22. [PubMed: 27624438]
7. Regatte RR, Akella SV, Lonner JH, Kneeland JB, Reddy R. T1rho relaxation mapping in human osteoarthritis (OA) cartilage: comparison of T1rho with T2. *J Magn Reson Imaging*. 2006;23:547–553. [PubMed: 16523468]
8. Li X, Benjamin Ma C, Link TM, et al. In vivo T(1rho) and T(2) mapping of articular cartilage in osteoarthritis of the knee using 3 T MRI. *Osteoarthritis Cartilage*. 2007;15:789–797. [PubMed: 17307365]
9. Takahashi K, Hashimoto S, Kiuchi S, et al. Bone morphological factors influencing cartilage degeneration in the knee. *Mod Rheumatol*. 2018;28:351–357. [PubMed: 28830272]
10. Russell C, Pedoia V, Amano K, Potter H, Majumdar S, Consortium A-A. Baseline cartilage quality is associated with voxel-based T1rho and T2 following ACL reconstruction: A multicenter pilot study. *J Orthop Res*. 2017;35:688–698. [PubMed: 27138363]
11. Teng HL, Pedoia V, Link TM, Majumdar S, Souza RB. Local associations between knee cartilage T1rho and T2 relaxation times and patellofemoral joint stress during walking: A voxel-based relaxometry analysis. *Knee*. 2018.
12. Peterfy CG, Guermazi A, Zaim S, et al. Whole-Organ Magnetic Resonance Imaging Score (WORMS) of the knee in osteoarthritis. *Osteoarthritis Cartilage*. 2004;12:177–190. [PubMed: 14972335]
13. Stefanik JJ, Niu J, Gross KD, Roemer FW, Guermazi A, Felson DT. Using magnetic resonance imaging to determine the compartmental prevalence of knee joint structural damage. *Osteoarthritis Cartilage*. 2013;21:695–699. [PubMed: 23428598]

14. Harada Y, Tokuda O, Fukuda K, et al. Relationship between the trochlear groove angle and patellar cartilage morphology defined by 3D spoiled gradient-echo imaging. *Skeletal Radiol.* 2012;41:589–594. [PubMed: 21898117]
15. Stefanik JJ, Roemer FW, Zumwalt AC, et al. Association between measures of trochlear morphology and structural features of patellofemoral joint osteoarthritis on MRI: the MOST study. *J Orthop Res.* 2012;30:1–8. [PubMed: 21710542]
16. Neogi T, Bowes MA, Niu J, et al. Magnetic resonance imaging-based three-dimensional bone shape of the knee predicts onset of knee osteoarthritis: data from the osteoarthritis initiative. *Arthritis Rheum.* 2013;65:2048–2058. [PubMed: 23650083]
17. Voss A, Shin SR, Murakami AM, et al. Objective quantification of trochlear dysplasia: Assessment of the difference in morphology between control and chronic patellofemoral instability patients. *Knee.* 2017;24:1247–1255. [PubMed: 28666647]
18. Widjajakim R, Roux M, Jarraya M, et al. Relationship of trochlear morphology and patellofemoral joint alignment to superolateral Hoffa fat pad edema on MR images in individuals with or at risk for osteoarthritis of the Knee: The MOST study. *Radiology.* 2017;284:806–814. [PubMed: 28418810]
19. Eijkenboom JJ, Waarsing JH, Lankhorst NE, Bierma-Zeinstra SM, van Middelkoop M. Statistical shape modelling of the patella: Patients with patellofemoral pain and patellofemoral osteoarthritis share similar aberrant shape aspects compared to healthy controls. *Osteoarthritis Cartilage.* 2016;24:S243–S244.
20. Gregory JS, Waarsing JH, Day J, et al. Early identification of radiographic osteoarthritis of the hip using an active shape model to quantify changes in bone morphometric features: can hip shape tell us anything about the progression of osteoarthritis? *Arthritis Rheum.* 2007;56:3634–3643. [PubMed: 17968890]
21. Baker-LePain JC, Lane NE. Relationship between joint shape and the development of osteoarthritis. *Curr Opin Rheumatol.* 2010;22:538–543. [PubMed: 20644480]
22. Hunter D, Nevitt M, Lynch J, et al. Longitudinal validation of periarticular bone area and 3D shape as biomarkers for knee OA progression? Data from the FNIH OA Biomarkers Consortium. *Ann Rheum Dis.* 2016;75:1607–1614. [PubMed: 26483253]
23. Stehling C, Liebl H, Krug R, et al. Patellar cartilage: T2 values and morphologic abnormalities at 3.0-T MR imaging in relation to physical activity in asymptomatic subjects from the osteoarthritis initiative. *Radiology.* 2010;254:509–520. [PubMed: 20019141]
24. Gersing AS, Schwaiger BJ, Nevitt MC, et al. Is weight loss associated with less progression of changes in knee articular cartilage among obese and overweight patients as assessed with MR imaging over 48 months? Data from the Osteoarthritis Initiative. *Radiology.* 2017;284:508–520. [PubMed: 28463057]
25. Pan J, Pialat J-B, Joseph T, et al. Knee cartilage T2 characteristics and evolution in relation to morphologic abnormalities detected at 3-T MR imaging: a longitudinal study of the normal control cohort from the Osteoarthritis Initiative. *Radiology.* 2011;261:507–515. [PubMed: 21900614]
26. Roos EM, Lohmander LS. The Knee injury and Osteoarthritis Outcome Score (KOOS): from joint injury to osteoarthritis. *Health Qual Life Outcomes.* 2003;1:64–64. [PubMed: 14613558]
27. Collins NJ, Misra D, Felson DT, Crossley KM, Roos EM. Measures of knee function: International Knee Documentation Committee (IKDC) Subjective Knee Evaluation Form, Knee Injury and Osteoarthritis Outcome Score (KOOS), Knee Injury and Osteoarthritis Outcome Score Physical Function Short Form (KOOS-PS), Knee Outcome Survey Activities of Daily Living Scale (KOS-ADL), Lysholm Knee Scoring Scale, Oxford Knee Score (OKS), Western Ontario and McMaster Universities Osteoarthritis Index (WOMAC), Activity Rating Scale (ARS), and Tegner Activity Score (TAS). *Arthritis Care Res (Hoboken).* 2011;63:208–228. [PubMed: 20862684]
28. Hawker GA, Mian S, Kendzerska T, French M. Measures of adult pain: Visual Analog Scale for Pain (VAS Pain), Numeric Rating Scale for Pain (NRS Pain), McGill Pain Questionnaire (MPQ), Short-Form McGill Pain Questionnaire (SF-MPQ), Chronic Pain Grade Scale (CPGS), Short Form-36 Bodily Pain Scale (SF-36 BPS), and Measure of Intermittent and Constant Osteoarthritis Pain (ICOAP). *Arthritis Care Res (Hoboken).* 2011;63:240–252. [PubMed: 20824800]

29. Shamonin D, Bron E, Lelieveldt B, Smits M, Klein S, Staring M. Fast parallel image registration on CPU and GPU for diagnostic classification of Alzheimer's disease. *Front Neuroinform.* 2014;7:50. [PubMed: 24474917]
30. Klein S, Staring M, Murphy K, Viergever MA, Pluim JPW. elastix: A toolbox for intensity-based medical image registration. *IEEE Trans Med Imaging.* 2010;29:196–205. [PubMed: 19923044]
31. Pedoia V, Li X, Su F, Calixto N, Majumdar S. Fully automatic analysis of the knee articular cartilage T1rho relaxation time using voxel-based relaxometry. *J Magn Reson Imaging.* 2016;43:970–980. [PubMed: 26443990]
32. Carballido-Gamio J, Bauer JS, Stahl R, et al. Inter-subject comparison of MRI knee cartilage thickness. *Med Image Anal.* 2008;12:120–135. [PubMed: 17923429]
33. Lansdown DA, Zaid M, Pedoia V, et al. Reproducibility measurements of three methods for calculating in vivo MR-based knee kinematics. *J Magn Reson Imaging.* 2015;42:533–538. [PubMed: 25545617]
34. Lombaert H, Grady L, Polimeni JR, Cheriet F. FOCUSR: feature oriented correspondence using spectral regularization--a method for precise surface matching. *IEEE Trans Pattern Anal Mach Intell.* 2013;35:2143–2160. [PubMed: 23868776]
35. Pedoia V, Lansdown DA, Zaid M, et al. Three-dimensional MRI-based statistical shape model and application to a cohort of knees with acute ACL injury. *Osteoarthritis Cartilage.* 2015;23:1695–1703. [PubMed: 26050865]
36. Pedoia V, Gallo MC, Souza RB, Majumdar S. Longitudinal study using voxel-based relaxometry: Association between cartilage T(1ρ) and T(2) and patient reported outcome changes in hip osteoarthritis. *J Magn Reson Imaging.* 2017;45:1523–1533. [PubMed: 27626787]
37. Marchini J, Presanis A. Comparing methods of analyzing fMRI statistical parametric maps. *Neuroimage.* 2004;22:1203–1213. [PubMed: 15219592]
38. Pedoia V, Samaan MA, Inamdar G, Gallo MC, Souza RB, Majumdar S. Study of the interactions between proximal femur 3d bone shape, cartilage health, and biomechanics in patients with hip Osteoarthritis. *J Orthop Res.* 2018;36:330–341. [PubMed: 28688198]
39. Jungmann PM, Tham S-C, Liebl H, et al. Association of trochlear dysplasia with degenerative abnormalities in the knee: data from the Osteoarthritis Initiative. *Skeletal Radiol.* 2013;42:1383–1392. [PubMed: 23801099]
40. Harbaugh CM, Wilson NA, Sheehan FT. Correlating femoral shape with patellar kinematics in patients with patellofemoral pain. *J Orthop Res.* 2010;28:865–872. [PubMed: 20108348]
41. Hefzy MS, Jackson WT, Saddemi SR, Hsieh YF. Effects of tibial rotations on patellar tracking and patello-femoral contact areas. *J Biomed Eng.* 1992;14:329–343. [PubMed: 1513139]
42. Powers CM, Ward SR, Chan LD, Chen YJ, Terk MR. The effect of bracing on patella alignment and patellofemoral joint contact area. *Med Sci Sports Exerc.* 2004;36:1226–1232. [PubMed: 15235330]
43. Kalichman L, Zhang Y, Niu J, et al. The association between patellar alignment and patellofemoral joint osteoarthritis features--an MRI study. *Rheumatology (Oxford).* 2007;46:1303–1308. [PubMed: 17525117]
44. Hunter DJ, Zhang YQ, Niu JB, et al. Patella malalignment, pain and patellofemoral progression: the Health ABC Study. *Osteoarthritis Cartilage.* 2007;15:1120–1127. [PubMed: 17502158]
45. Liao TC, Yang N, Ho KY, Farrokhi S, Powers CM. Femur rotation increases patella cartilage stress in females with patellofemoral pain. *Med Sci Sports Exerc.* 2015;47:1775–1780. [PubMed: 25606814]
46. Liao TC, Yin L, Powers CM. The influence of isolated femur and tibia rotations on patella cartilage stress: A sensitivity analysis. *Clinical Biomechanics.* 2018;12:125–131.
47. Baldwin JL, House CK. Anatomic dimensions of the patella measured during total knee arthroplasty. *J Arthroplasty.* 2005;20:250–257. [PubMed: 15902866]
48. van Middelkoop M, Macri EM, Eijkenboom JF, et al. Are Patellofemoral Joint Alignment and Shape Associated With Structural Magnetic Resonance Imaging Abnormalities and Symptoms Among People With Patellofemoral Pain? *Am J Sports Med.* 2018;46:3217–3226. [PubMed: 30321064]

49. Crossley KM, Macri EM, Cowan SM, Collins NJ, Roos EM. The patellofemoral pain and osteoarthritis subscale of the KOOS (KOOS-PF): development and validation using the COSMIN checklist. *Br J Sports Med.* 2017.
50. Mehl J, Feucht MJ, Bode G, Dovi-Akue D, Südkamp NP, Niemeyer P. Association between patellar cartilage defects and patellofemoral geometry: a matched-pair MRI comparison of patients with and without isolated patellar cartilage defects. *Knee Surgery, Sports Traumatology, Arthroscopy.* 2016;24:838–846.

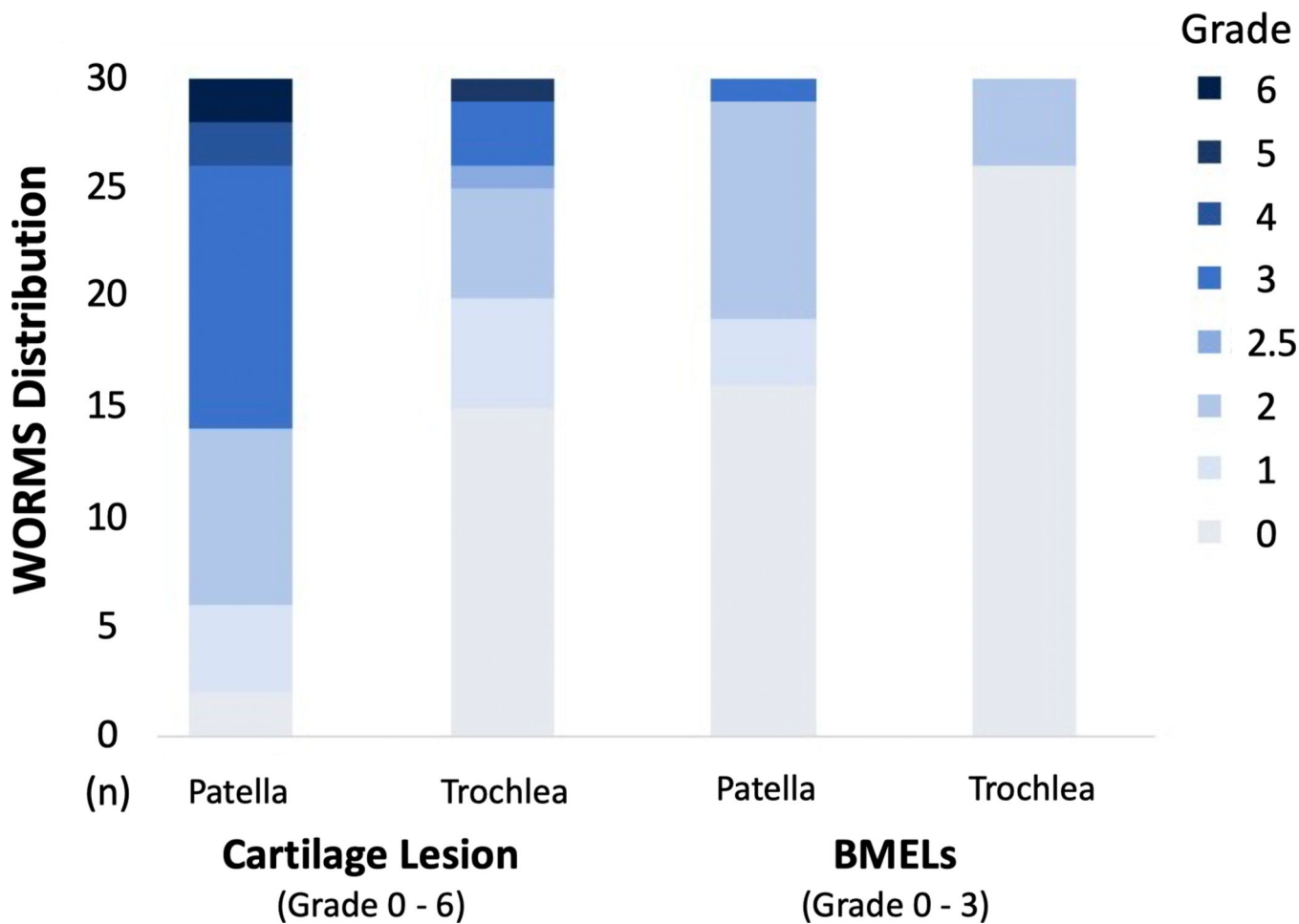


Figure 1. Distribution of the morphological grading of the cartilage and bone marrow edema-like lesions (BMELs) using the whole organ magnetic resonance imaging score (WORMS). Only subjects who were classified in the patellofemoral joint degeneration group are shown here (number of subjects [n] = 30).

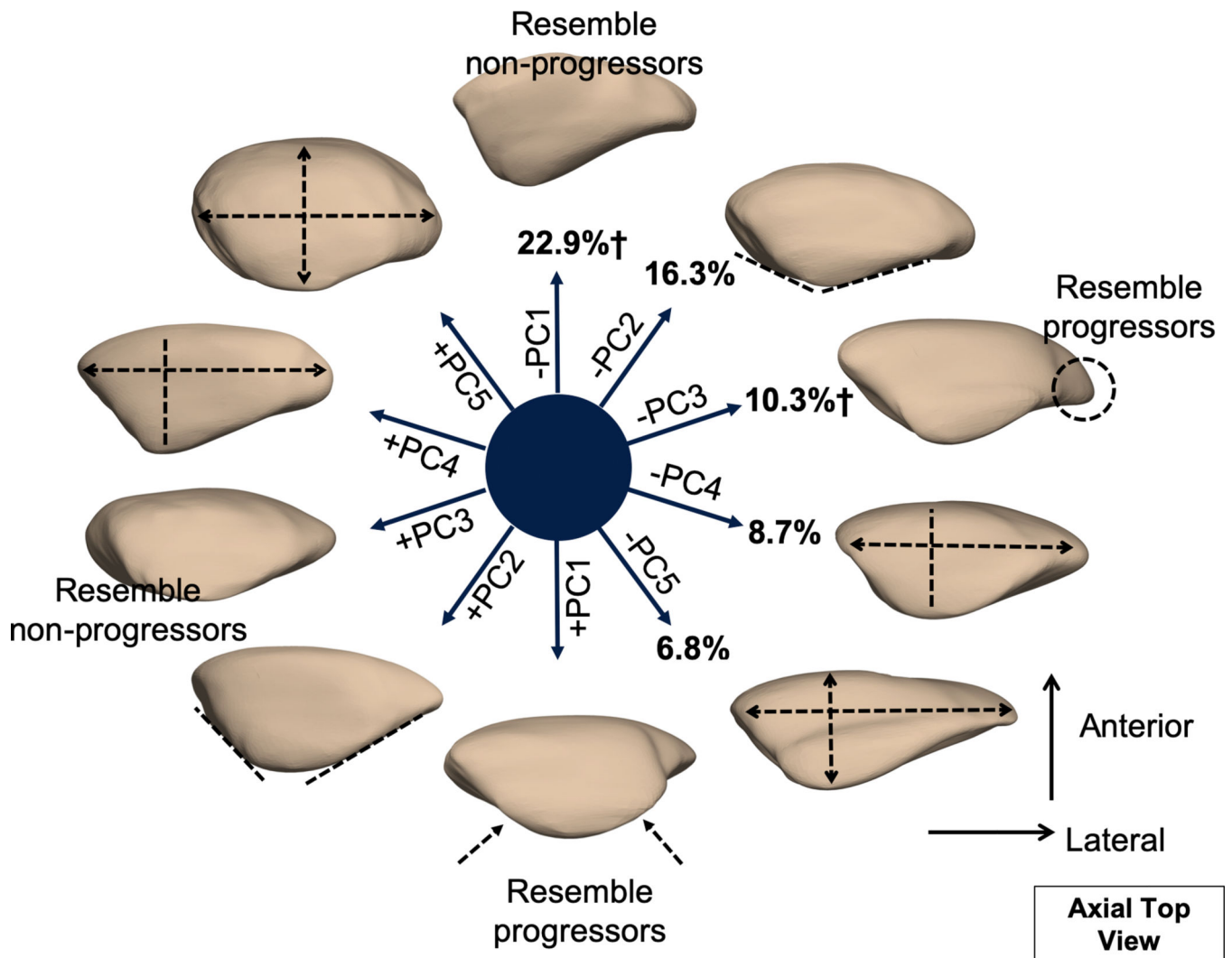


Figure 2.

Illustration of the first 5 patella principal component (PC) modes. Each mode is visualized at mean \pm 3 mode variance. The percentage indicates the percent variance explained by each mode. Mode 1 and mode 3 were significant predictors of the worsening of patellofemoral joint morphological features over 3 years. Subjects who exhibited progression exhibited a patella with equally distributed facets (mode 1) and a patella with lateral bump or hook (mode 3).

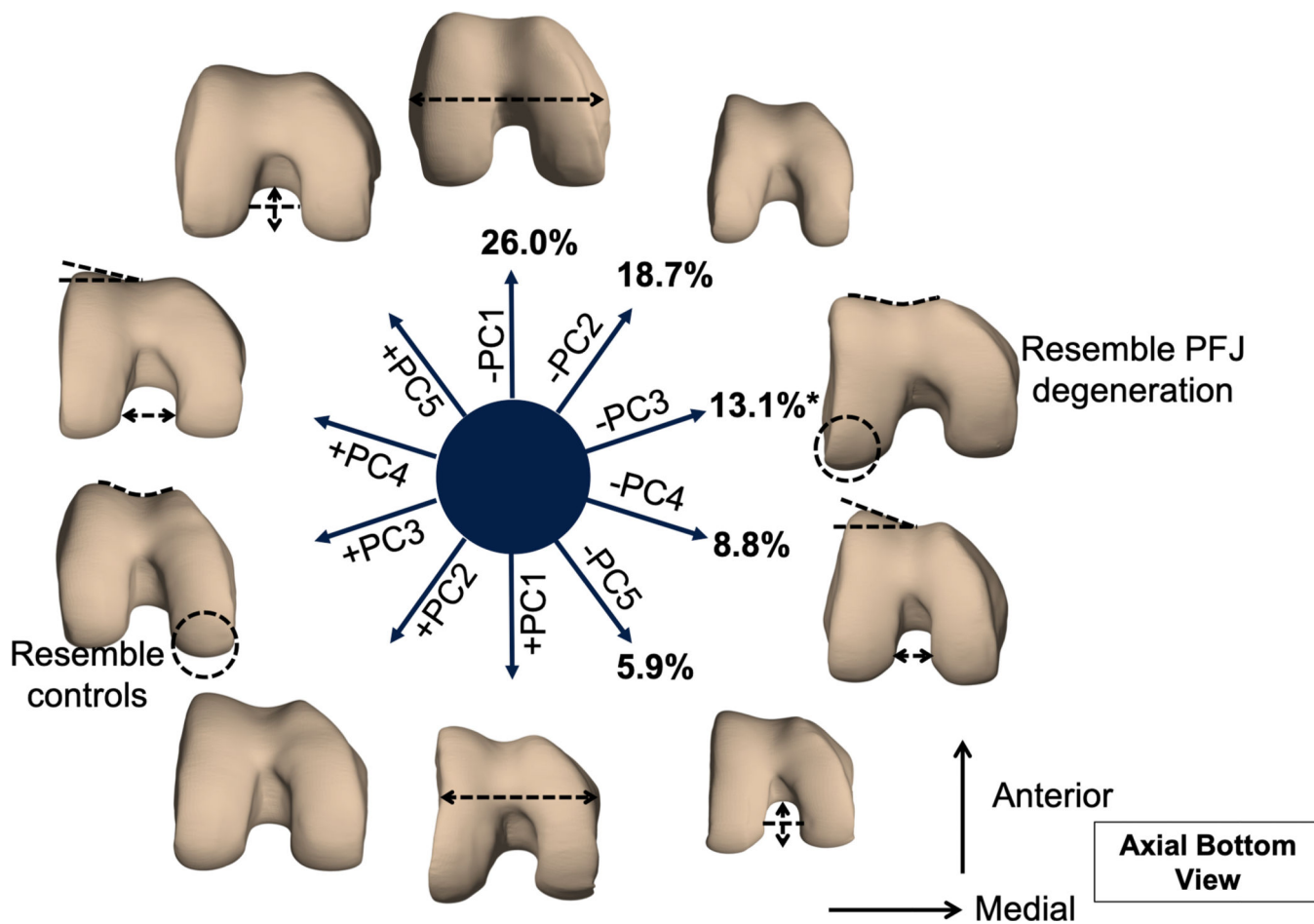


Figure 3. Illustration of the first 5 trochlear principal component (PC) modes. Each mode is visualized at mean \pm 3 mode variance. The percentage indicates the percent variance explained by each mode. Mode 3 was significant predictor of the presence of patellofemoral joint (PFJ) degeneration at baseline. Subjects with PFJ degeneration exhibited a trochlea with longer lateral condyle and shallower trochlear groove.

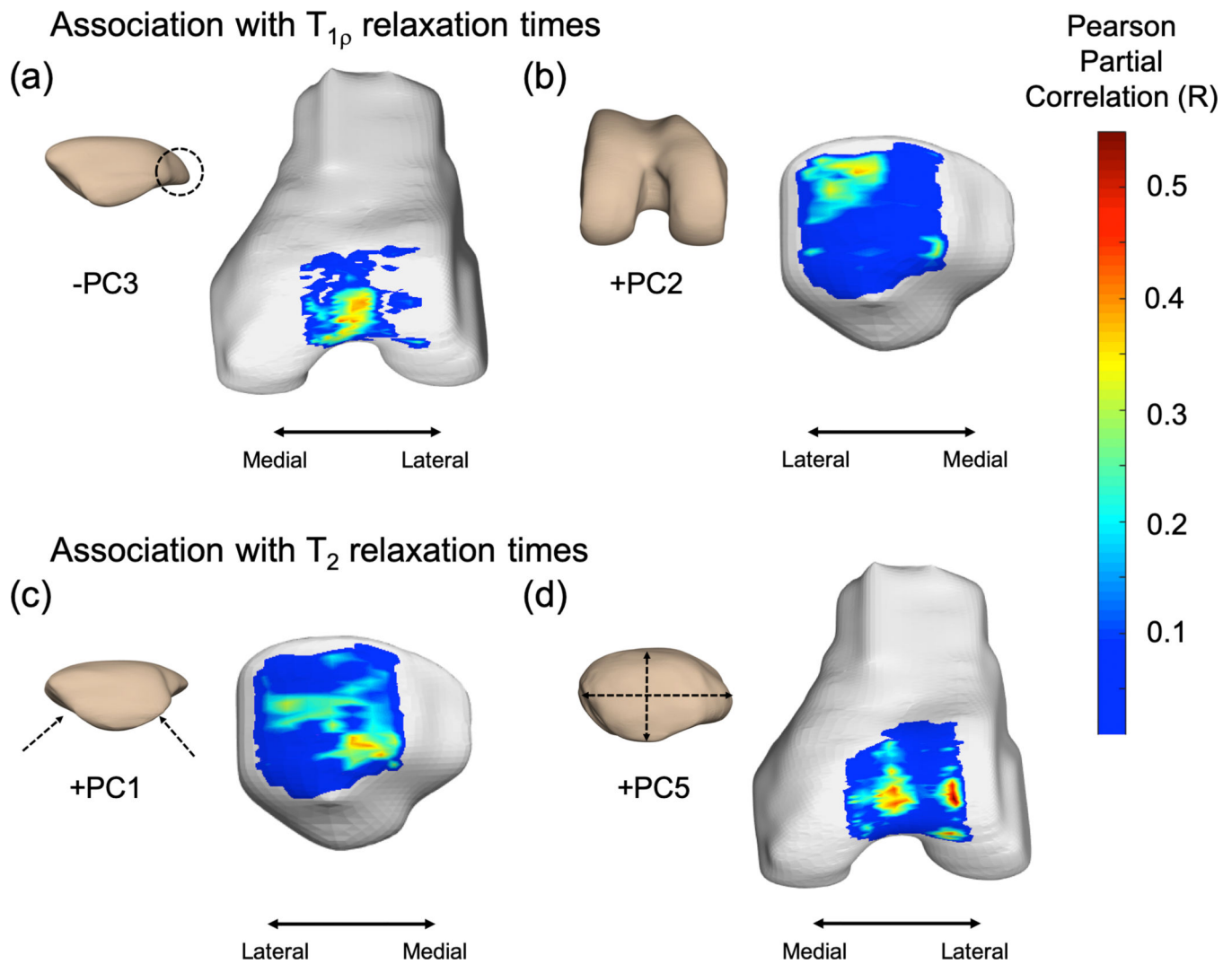


Figure 4.

Statistical parametric mapping of Pearson partial correlations between bone shape features and cartilage relaxation times. Elevated $T_{1\rho}$ was associated with (a) lower patella PC3 score (percent significant voxels (PSV) = 10.2%, average $R = -0.39$, average $p = 0.020$) and (b) greater trochlea PC2 score (PSV = 12.8%, $R = 0.38$, $p = 0.025$). Elevated T_2 was associated with (c) greater patella PC1 (PSV = 10.5%, $R = 0.43$, $p = 0.019$) and (d) greater PC5 scores (PSV = 13.3%, $R = 0.46$, $p = 0.015$).

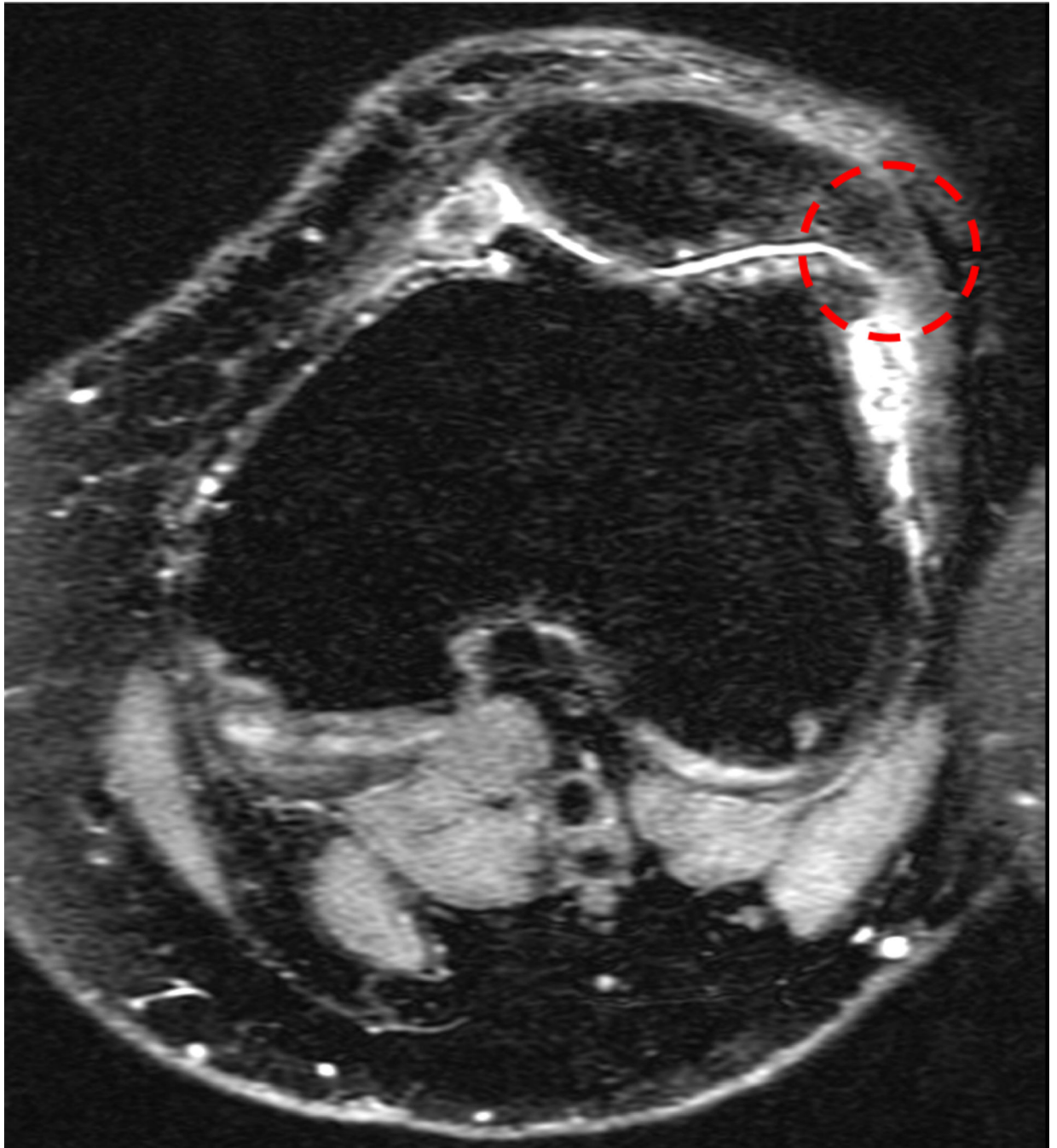


Figure 5. Example of a patella featuring lateral bump or hook that resembles an osteophyte or exostosis associated with patellofemoral joint degeneration. Representation of axial patellofemoral joint image of a subject with lowest patella – mode 3.

Table 1.

Baseline demographics and patient-reported symptoms in the patellofemoral joint (PFJ) degeneration and control groups.

	PFJ degeneration (n=30)	Control (n=23)	p value
Demographics			
Sex, n [‡]	6 males, 24 females	12 males, 11 females	0.020
Age, y	53.2 ± 9.8	48.1 ± 10.6	0.078
Body mass index, kg/m ²	23.8 ± 3.2	23.9 ± 3.0	0.923
KOOS[‡] (0 – 100)			
Pain	91.6 (83.3 – 100.0)	97.2 (93.7 – 100.0)	0.097
Symptoms	92.8 (85.7 – 96.4)	96.4 (89.2 – 100.0)	0.093
Daily activity	97.0 (91.1 – 100.0)	98.5 (96.6 – 100.0)	0.065
Sports	90.0 (80.0 – 100.0)	90.0 (85.0 – 100.0)	0.324
Quality of life	87.5 (73.4 – 100.0)	90.6 (75.0 – 100.0)	0.645

Age and body mass index presented as mean ± SD, KOOS presented as median (IQR). Abbreviations: KOOS, Knee Injury and Osteoarthritis Outcome Score.

[‡]Indicates chi-square analysis

[‡]indicates Mann-Whitney U test.